

Multi-Layer Optical Coatings Composed of Silicon Nanoparticles

By

Kari Sanford

Has been approved

April 2017

APPROVED (printed name, signature):

Zachary Holman, **Director**

William Weigand, **Second Reader**

ACCEPTED:

Dean, Barrett, the Honors College

ABSTRACT

To compete with fossil fuel electricity generation, there is a need for higher efficiency solar cells to produce renewable energy. Currently, this is the best way to lower generation costs and the price of energy [1].

The goal of this Barrett Honors Thesis is to design an optical coating model that has five or fewer layers (with varying thickness and refractive index, within the above range) and that has the maximum reflectance possible between 950 and 1200 nanometers for normally incident light.

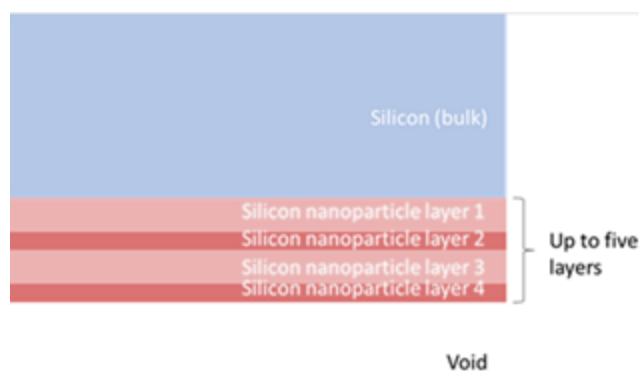


Figure 0.1 Optical Coating Example Model

Manipulating silicon monolayers to become efficient inversion layers to use in solar cells aligns with the Ira. A Fulton Schools of Engineering research themes of energy and sustainability [2]. Silicon monolayers could be specifically designed for different doping substrates. These substrates could range from common-used materials such as boron and phosphorus, to rare-earth doped zinc oxides or even fullerene blends. Exploring how the doping material, and in what quantity, affects solar cell energy output could revolutionize the current production methods and commercial market. If solar cells can be manufactured more economically, yet still retain high efficiency rates, then more people will have access to alternate, “green” energy that does not deplete nonrenewable resources.

ACKNOWLEDGEMENTS

First and foremost, I would like to thank two incredible advisors, Dr. Zachary Holman and William Weigand, who have mentored me through this project. This research opportunity has sparked academic enlightenment and personal growth. I am incredibly thankful to two graduate students who aided in deposition work, Jonathan Bryan and Peter Firth. I would like to thank Jason Yu for training me on the Essential Macleod software. I am grateful for the guidance I received in spectrophotometry analysis methods from Salman Manzoor. I would like to thank Joe Carpenter and Mathieu Boccard for welcoming me into the Holman Lab, introducing me to colleagues, training me on the machines, and sharing relevant literature and resources. I want to acknowledge Nathan Rodkey for challenging me to produce the best work possible. I would like to thank my family for their love and encouragement during this research project. It is my hope that the silicon nanoparticle samples provide a better understanding of how Bragg reflectors absorb and reflect light. The different data sets also provide insight to how the Holman Lab's Deposition Tool can be modified to create more uniform, replicable samples for future projects.

TABLE OF CONTENTS

CHAPTER	PAGE
List of Figures	5
List of Tables	7
List of Equations	8
Chapter 1: Introduction	9
Chapter 2: Macleod Software	12
2.1 How It Works: Macleod Software	12
2.2 Methods	12
2.3 Virtual Models	15
2.4 Lessons Learned	18
Chapter 3: Deposition Tool	19
3.1 How It Works: Deposition Tool	19
3.2 Methods	19
3.3 Results	21
3.4 Lessons Learned	25
Chapter 4: Ellipsometry Analysis	26
4.1 How It Works: Ellipsometer	26
4.2 Methods	27
4.3 Results	28
4.4 Conclusion	32
4.5 Lessons Learned	32
Chapter 5: Spectrophotometry Analysis	33
5.1 How It Works: Spectrophotometer	33
5.2 Methods	34
5.3 Results	34
5.4 Conclusion	36
5.5 Lessons Learned	36
Chapter 6: Future Work	38
Chapter 7: Conclusion	39
References	40

LIST OF FIGURES

FIGURE	PAGE
Figure 0.1 Optical Coating Example Model	2
Figure 1.1 Refraction of a light beam [7]	10
Figure 1.2 Absorber of a p-n Junction Silicon Solar Cell [8]	11
Figure 2.1 Broad-band-pass filter [3]	12
Figure 2.2 Refraction tilts the transmitted beam [3]	14
Figure 2.3 Silicon Nanoparticle Monolayer, Refractive Index 1.35	15
Figure 2.4 Silicon Nanoparticle Monolayer, Refractive Index 1.46	16
Figure 2.5 Silicon Nanoparticle Monolayer, Refractive Index 1.13	17
Figure 2.6 Silicon Nanoparticle Double Layer Optical Coating, Alternating	17
Figure 2.7 Silicon Nanoparticle Multi-Layer Optical Coating, Alternating	17
Figure 2.8 Silicon Nanoparticle Multi-Layer Optical Coating, BAD MODEL	18
Figure 3.1 Single Layer Samples: Difference in Thickness	22
Figure 3.2 Double Layer Samples: Difference in Thickness	22
Figure 3.3 Single Layer Samples: Difference in Porosity	23

FIGURE	PAGE
Figure 3.4 Double Layer Samples: Difference in Porosity	23
Figure 3.5 Single Layer Samples: Difference in Refractive Index	24
Figure 3.6 Double Layer Samples: Difference in Refractive Index	24
Figure 4.1 Digital Model of M-2000 J.A. Woollam Co. Ellipsometer	26
Figure 4.2 Nulling Ellipsometer Schematic [16]	27
Figure 4.3 Ellipsometry Analysis of Silicon Nanoparticle Monolayer	28
Figure 4.4 Ellipsometry Analysis of Silicon Nanoparticle Multi-Layer	29
Figure 5.1 Top Down View of the Lambda 950 Spectrophotometer [21]	33
Figure 5.2 Reflectance Correction Settings in the Integrating Sphere	34
Figure 5.3 Silicon Nanoparticle Monolayer Reflectance Values	35
Figure 5.4 Silicon Nanoparticle Multi-Layer Reflectance Values	35

LIST OF TABLES

TABLE	PAGE
Table 3.1 Deppy Settings, Final Batch	20
Table 4.1 Thickness: Expected versus Result	30
Table 4.2 Porosity: Expected versus Result	30
Table 4.3 Refractive Index: Expected versus Result	31
Table 4.4 Thickness Difference: Result – Expected	31
Table 4.5 Porosity Difference: Result – Expected	31
Table 4.6 Refractive Index Difference: Result – Expected	32

LIST OF EQUATIONS

EQUATION	PAGE
Equation 1.1 Index of Refraction Definition [7]	10
Equation 2.1 Reflectance Definition	13
Equation 2.2 Transmittance Definition	13
Equation 2.3 Amplitude Reflection Coefficient	14

CHAPTER 1: INTRODUCTION

In efforts to increase the electrical current of solar cells, the objective of this investigation was to design optical coatings, thin layers of material, made with silicon nanoparticle layers. Optical coatings are usually the top layer(s) of a surface. The surface could be made of multiple materials stacked on top of each other, each layer separated by an interface [3]. The properties of this surface are specular, meaning, “The directions of light obey the laws of reflection and refraction, and their shape is adjusted to direct the light in a desired manner” [3]. However, the reflectance, transmittance, and phase change properties of a given surface are poor. The purpose of optical coatings is to improve the above properties of a surface without changing its specular behavior [3].

The optical coating must have five or fewer layers in order to modify the spectral reflection and transmission of the silicon wafer without altering the physical or optical properties in a way that decreases absorption [4]. Considering that the refractive index, ratio of the velocity of light in vacuum to its velocity in a specified medium, of silicon nanoparticle films can range from about 1.1 to 1.4, the optical coating must have this characteristic to achieve the maximum reflectance possible between 950 and 1200 nm for normally incident light [5].

The project optical coating designs were made in the Macleod software, a program that simulates and manipulates virtual models. The simulation has the light start in a semi-infinite silicon slab, onto which the coating would be deposited. Once the virtual model of the optical coating met the specifications of the project goals, the optical coatings were created using a deposition tool. Silicon nanoparticles were synthesized with a plasma process in which the SiH_4 molecules are decomposed, and small spheres (nanoparticles) are nucleated [6]. Then, the sample was analyzed with both ellipsometry and UV-Vis-NIR spectrophotometry methods to determine

if the layers have the target thicknesses and refractive indices, and if the coating reflects light as simulated.

Another goal in this thesis project was to determine the thickness and refractive index of each of the layers from a single ellipsometry measurement. Refractive index is defined as the ratio of the velocity of light in a vacuum to the velocity of light in a medium [7].

$$\frac{\sin \alpha}{\sin \beta} = \frac{c_{vac}}{c_{med}} = n = \frac{c}{v}$$

Equation 1.1 Index of Refraction Definition [7]

“The magnitude of the refractive index depends on the wavelength of the incident light. This property is called dispersion” [7]. To keep results consistent across different samples, the wavelength range is 950 to 1200 nm [3]. When light travels from a vacuum to a medium (or incident), the velocity and wavelength will decrease to keep the energy rate constant [7].

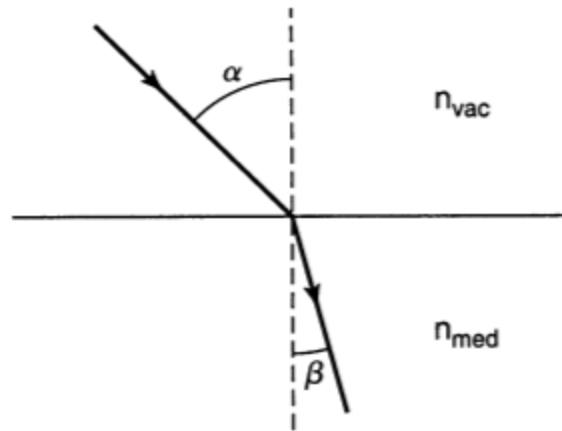


Figure 1.1 “Refraction of a light beam when traversing the boundary from an optically thin medium into an optically denser medium [7]

This project will determine which refractive index value will yield the best performance parameters.

There was a preliminary experiment in which two layers were deposited—one very dense and one more porous—with witness samples for each of the two depositions. Thickness and refractive index of the layers were measured individually, and the deposition tool recipes tried reproduce the same thicknesses and refractive indices when the two layers were stacked.

The thickness and density values of the samples were used to determine how to “seed” the growth of crystalline silicon thin films, regardless of the underlying substrate. Thin, crystalline silicon layers will form a p-n junction with the silicon wafer, which forms the absorber of a solar cell [8]. These layers are more effective at coupling light into the wafer—where it is absorbed—if they are crystalline. This crystalline form is what the nanoparticle seed layer has facilitated.

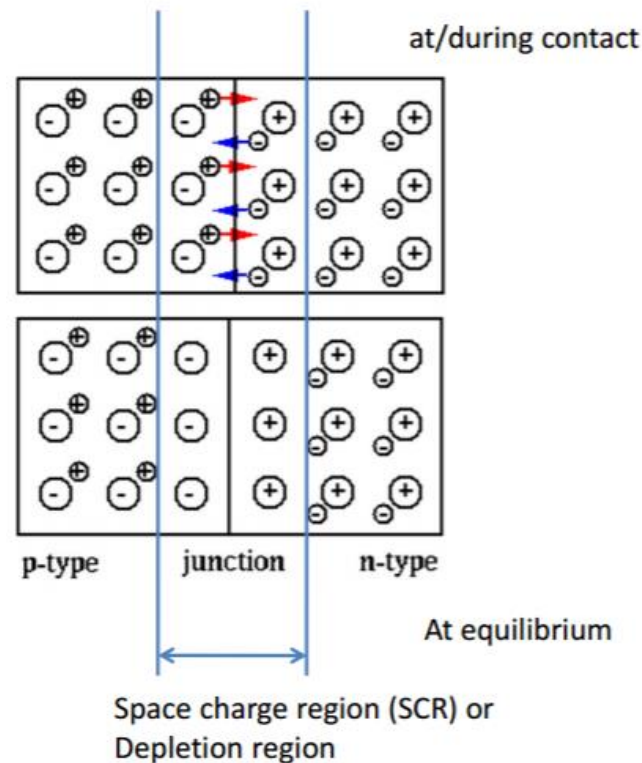


Figure 1.2 Absorber of a p-n Junction Silicon Solar Cell [8]

CHAPTER 2: MACLEOD VIRTUAL SIMULATION SOFTWARE

2.1 HOW IT WORKS: MACLEOD SOFTWARE

The Macleod software creates virtual models that are stacks of thin films, or optical coatings. These optical coatings can either decrease reflectance and increase transmittance or increase reflectance and decrease transmittance for all of a surface, or just a portion of it [3]. In a model of silicon nanoparticle thin-film assembly, or multilayers, the amount of light reflected by the surface and its coatings depends on the refractive index of each layer. The amount of light absorbed by the multilayer coating depends on both the refractive index and the thickness of each layer. These two parameters, refractive index and thickness, can be manipulated in the software to simulate different absorption and reflection values for each layer in a multilayer coating.

2.2 METHODS

Given previous performance data, the Macleod software can generate multi-layer optical coating recipes to achieve greater performances. The performance parameters are wavelength, reflectance, transmittance, and incidence angle.

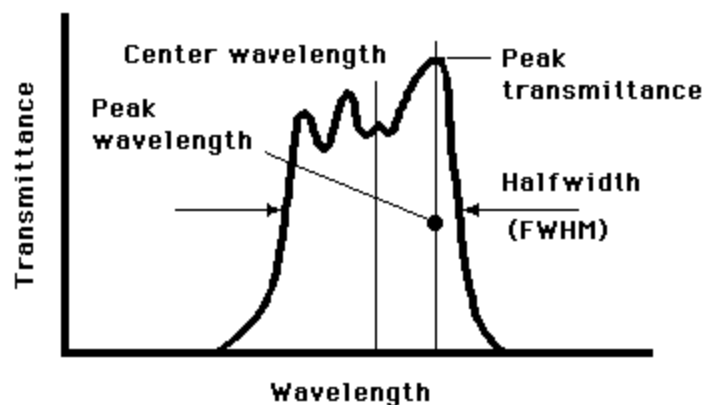


Figure 2.1 “A broad-band-pass filter of idealized design defining the principal terms used for describing the optical characteristic” [3].

Recall that the wavelength range for maximum reflectance of silicon nanoparticle layers in normally incident light is 950 to 1200 nm [5]. For this experiment, the wavelength range was 510 to 1600 nm. This large range encompassed both normally incident light, and all other light through terminal wavelength.

Reflectance and transmittance are “ratios of the components of irradiance, or intensity, normal to the surfaces of the films” [3]. These definitions are set because the area of the beam is larger than that of the receiver. This causes the total beam power to be measured, and the receiver is aligned normal to the beam [3].

$$R = \frac{\text{Irradiance Reflected Normally}}{\text{Irradiance Incident Normally}}$$

Equation 2.1 Reflectance Definition

$$T = \frac{\text{Irradiance Transmitted Normally}}{\text{Irradiance Incident Normally}}$$

Equation 2.2 Transmittance Definition

Incidence angle is defined as the angle at which the beam hits the sample, or incident boundary. At this angle, there is a difference in polarized state of the reflected and transmitted beams. There are two such states where the electric and magnetic field components are in the same plane. *P*-polarized light has the electric vector parallel to the plane of incidence [3]. *S*-polarized light has the electric vector perpendicular to the plane of incidence [3].

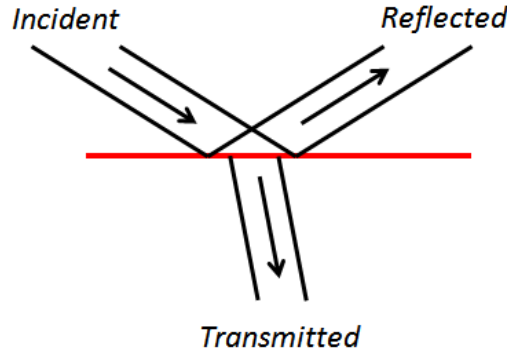


Figure 2.2 Refraction tilts the transmitted beam with respect to the incident beam. The beams span over different areas at the incident boundary [3].

“The normal components of irradiance used in the definitions of reflectance and transmittance are calculated using the components of the electric and magnetic fields of the waves which are parallel to the interfaces, that is the tangential components” [3]. These components are used in the definitions of amplitude reflection coefficient, ρ , and amplitude transmission coefficient, τ . Thin-films, and this experiment, will use components instead of the actual amplitude values [3].

$$\rho = \frac{\text{Reflected Amplitude (Tangential Component)}}{\text{Incident Amplitude (Tangential Component)}}$$

Equation 2.3 Amplitude Reflection Coefficient

$$\tau = \frac{\text{Transmitted Amplitude (Tangential Component)}}{\text{Incident Amplitude (Tangential Component)}}$$

Equation 2.4 Transmitted Reflection Coefficient

This experiment utilized the Macleod software to manipulate the thickness of a single silicon nanoparticle layer to achieve reflectance values that yielded either a high refractive index (approximately 1.35), or low refractive index (approximately 1.1). Once the reflectance values

were identified for each refractive index, the performance properties were saved to a layer. Next, silicon nanoparticle multi-layer models were simulated in Macleod, with the goal of using a combination of layers to achieve a high net reflectance value.

2.3 VIRTUAL MODELS

The figures below are screenshots of virtual models built and simulated in the Macleod software. The first models are single layers (monolayers) of silicon nanoparticles on a medium of crystalline silicon wafers. Once the software has successfully created several different monolayers of varying thicknesses and refractive indices, then these layers can be added to each other to create multi-layer stacks.

01Layer_Si_1.35RI

Design

Context

Notes

Incident Angle (deg)	0.00
Reference Wavelength (nm)	510.00

	Layer	Material	Refractive Index	Extinction Coefficient	Optical Thickness (FWOT)	Physical Thickness (nm)
	Medium	Si (CRYSTAL)	4.18125	0.10125		
▶	1	ZVar 20_ Dist 02	1.35364	0.00018	0.53083765	200.00
	Substrate	Air	1.00000	0.00000		

Figure 2.3 Silicon Nanoparticle Monolayer, Refractive Index 1.35

01Layer_Si based on 12.15.16 Results

Design | Context | Notes

Incident Angle (deg)	0.00					
Reference Wavelength (nm)	510.00					
	Layer	Material	Refractive Index	Extinction Coefficient	Optical Thickness (FWOT)	Physical Thickness (nm)
	Medium	Si (CRYSTAL)	4.18125	0.10125		
▶	1	Si hi n	1.45918	0.00027	0.46636377	163.00
	Substrate	Air	1.00000	0.00000		

Figure 2.4 Silicon Nanoparticle Monolayer, Refractive Index 1.46

01Layer_Si_1.13RI

Design

Context

Notes

Incident Angle (deg)	0.00					
Reference Wavelength (nm)	510.00					

	Layer	Material	Refractive Index	Extinction Coefficient	Optical Thickness (FWOT)	Physical Thickness (nm)
	Medium	Si (CRYSTAL)	4.18125	0.10125		
▶	1	ZVar 8_ Dist 14	1.13615	0.00005	0.44554706	200.00
	Substrate	Air	1.00000	0.00000		

Figure 2.5 Silicon Nanoparticle Monolayer, Refractive Index 1.13

02Layers_Si on Si						
Design Context Notes						
Incident Angle (deg)			0.00			
Reference Wavelength (nm)			510.00			
	Layer	Material	Refractive Index	Extinction Coefficient	Optical Thickness (FWOT)	Physical Thickness (nm)
	Medium	Si (CRYSTAL)	4.18125	0.10125		
	1	ZVar 8_Dist 14	1.13615	0.00005	0.16708015	75.00
▶	2	ZVar 20_Dist 02	1.35364	0.00018	0.33177353	125.00
	Substrate	Air	1.00000	0.00000		
					0.49885368	200.00

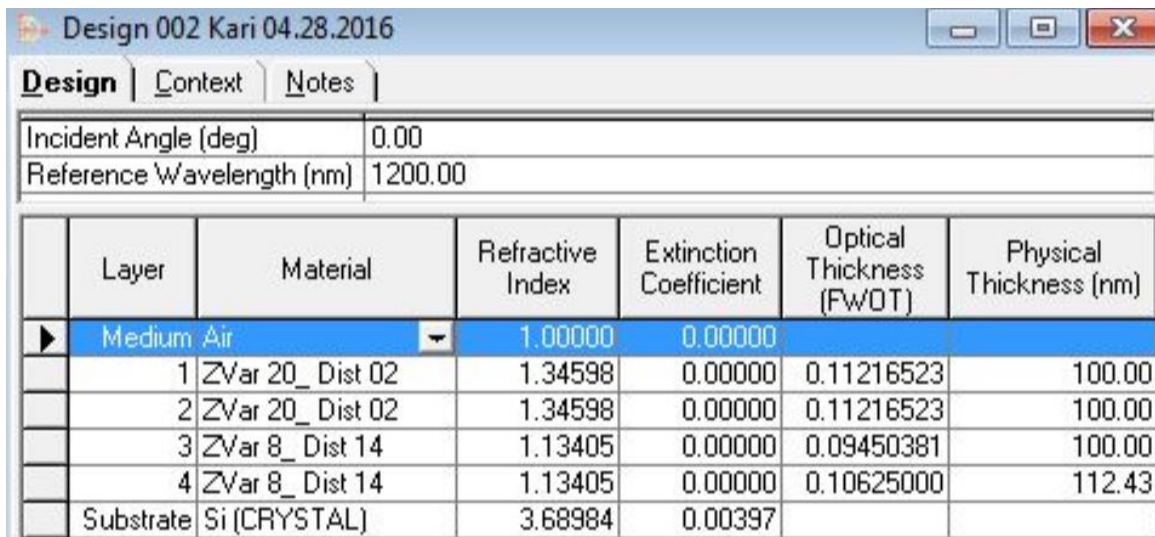
Figure 2.6 Silicon Nanoparticle Double Layer Optical Coating, Alternating Layers

Design003 05-26-2016						
Design Context Notes						
Incident Angle (deg)			0.00			
Reference Wavelength (nm)			900.00			
	Layer	Material	Refractive Index	Extinction Coefficient	Optical Thickness (FWOT)	Physical Thickness (nm)
	Medium	Si (CRYSTAL)	3.80889	0.02778		
	1	ZVar 8_Dist 14	1.13615	0.00005	0.29582783	234.34
	2	ZVar 20_Dist 02	1.35364	0.00018	0.29607950	196.86
	3	ZVar 8_Dist 14	1.13615	0.00005	0.29593941	234.43
▶	4	ZVar 20_Dist 02	1.35364	0.00018	0.29653775	197.16
	Substrate	Air	1.00000	0.00000		
					1.18438449	862.79

Figure 2.7 Silicon Nanoparticle Multi-Layer Optical Coating, Alternating Layers

2.4 LESSONS LEARNED

- **Identify the material of each layer in the model.** This includes the medium (bottom-most layer) and the substrate (top layer).
- **Specify the refractive index for each layer.** The assumed refractive index value is zero, which yields zero thickness. This generates an error message in the Macleod software.
- **Double check all parameters before generating designs or plots.** This ensures accurate simulation, and prevents error messages.
- **Use alternating layers in the model.** Stacking two of the same layer is the same as one very thick layer.
- **Minimize the number of layers used in the model.** “The total number of layers which it is possible to use is very large, but the greater the number of layers the more complicated the production procedure, and the greater the probability of an unacceptable error, so that the simpler designs are more attractive” [3].



Design 002 Kari 04.28.2016						
Design Context Notes						
Incident Angle (deg)		0.00				
Reference Wavelength (nm)		1200.00				
	Layer	Material	Refractive Index	Extinction Coefficient	Optical Thickness (FWOT)	Physical Thickness (nm)
▶	Medium	Air	1.00000	0.00000		
	1	ZVar 20_Dist 02	1.34598	0.00000	0.11216523	100.00
	2	ZVar 20_Dist 02	1.34598	0.00000	0.11216523	100.00
	3	ZVar 8_Dist 14	1.13405	0.00000	0.09450381	100.00
	4	ZVar 8_Dist 14	1.13405	0.00000	0.10625000	112.43
	Substrate	Si (CRYSTAL)	3.68984	0.00397		

Figure 2.8 Silicon Nanoparticle Multi-Layer Optical Coating, BAD MODEL

ERRORS: same layers stacked, and medium and substrate materials are incorrect.

CHAPTER 3: DEPOSITION TOOL

3.1 HOW IT WORKS: DEPOSITION TOOL

The deposition tool, or Deppy, operates using Hypersonic Particle Deposition (HPD) [9]. This process is independent of the nanomaterial or substrate properties. The HPD system deposits material in solution or synthesized in its plasma chamber, according to the procedure below [9].

1. User loads the substrate through an oxygen free environment (chamber).
2. The door seals. The chamber is brought under vacuum (approximately 25 mTorr).
3. Aerosolized particles enter the reaction chamber. Plasma treatment can occur here, under the discretion of the user.
4. “As aerosol flows through the system, the nozzle causes a 5-40X pressure drop between the reaction and deposition chambers” [9].
5. Nanoparticles exit the nozzle and enter the deposition chamber at a final velocity of 1 km/sec [9].
6. A substrate is translated through a curtain, into the deposition chamber. The high velocity particles impact and stick to the substrate. “The final thickness of the films is determined by the number of passes and the translation speed” [9].
7. “After the process is complete, the chamber is evacuated and the substrate removed. The end result is a uniformly coated substrate” [9].

3.2 METHODS

Hydrogenated microcrystalline silicon ($\mu\text{c-Si:H}$) [10, 11] is the most commonly used material in silicon-based thin-film solar cells [12] and microcrystalline/amorphous silicon solar cells [13]. The deposition tool was used to create the hydrogenated microcrystalline silicon

samples by depositing “plasma enhanced vapor deposition (PECVD), from a gas mixture of silane and hydrogen” [14] on top of silicon wafers.

The initial batches of silicon nanoparticle samples were created to determine machine efficiency. The same recipe was used for five samples, with the objective of creating five samples with identical performance parameters. This was not achieved in the first batch. The deposition tool settings were adjusted until the performance parameters’ expected values (Deppy recipe) matched the result values. Once samples consistently performed to expectation, the final batch of silicon nanoparticle samples were created. This final batch was used to achieve the project goal.

The table below illustrates the deposition tool settings used to produce samples of the final batch of the experiment. The shading in the table represents how the settings are grouped in the tool’s user interface.

Deppy Setting	Numerical Input, Dense Sample	Numerical Input, Porous Sample
Silane	300 sccm	300 sccm
Helium	250 sccm	250 sccm
Nitrogen	0 sccm	0 sccm
RN Pressure Read	1900 mTorr	1900 mTorr
DpC Pressure Read	200 mTorr	280 mTorr
Number of Loops	20	20
Speed	100	100
Z Position	-5	-5
Nozzle Width	1 mm	1 mm

Table 3.1 Deppy Settings, Final Batch

3.3 RESULTS

Samples 6 and 14 are dense, single layer samples. Samples 9 and 13 are porous, single layer samples. Samples 7 and 8 are dense on top of porous (multi-layer) samples, with sample 13 as the witness. Samples 11 and 12 are porous on top of dense (multi-layer) samples, with sample 14 as the witness. The scatter plots below illustrate the difference between expected (recipe) values and the results after ellipsometry analysis.

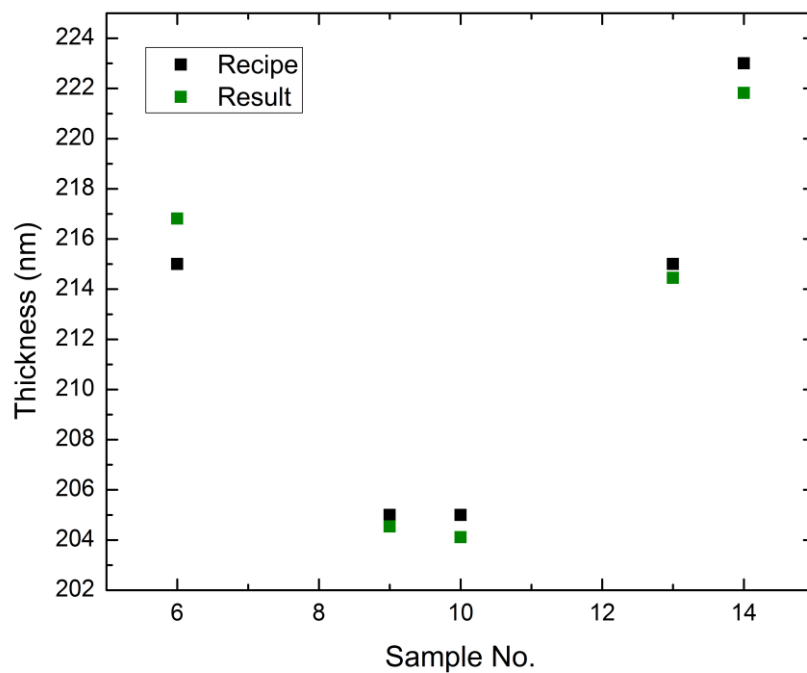


Figure 3.1 Single Layer Samples: Difference in Thickness

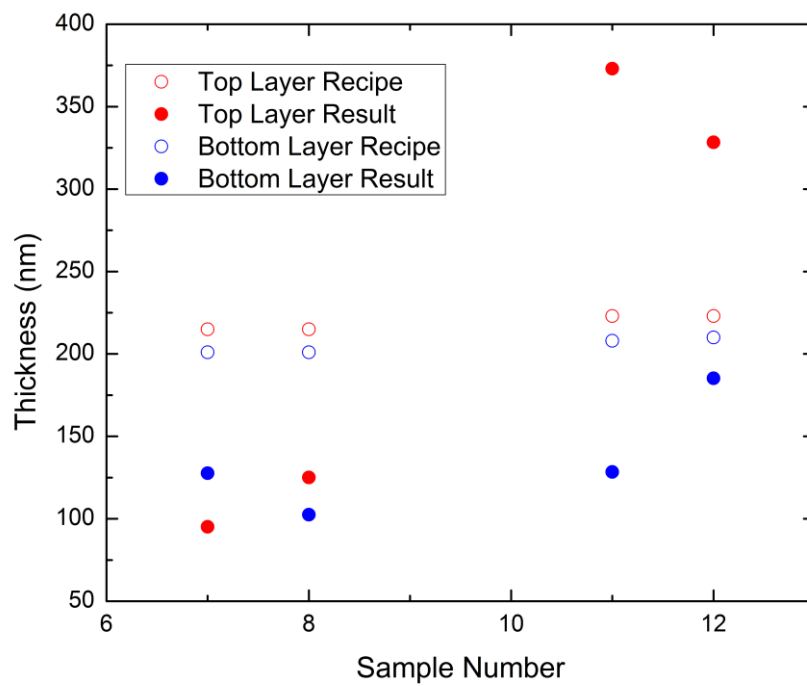


Figure 3.2 Double Layer Samples: Difference in Thickness

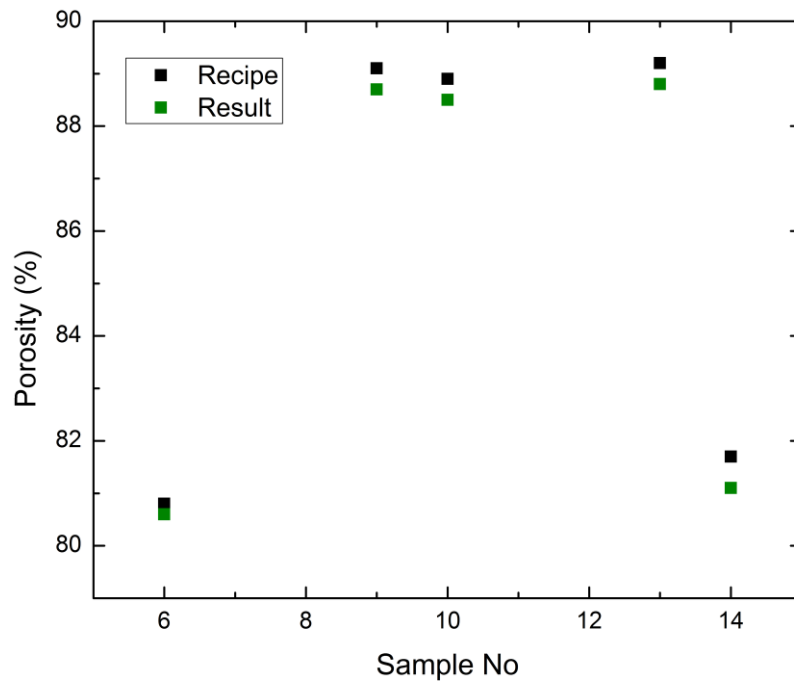


Figure 3.3 Single Layer Samples: Difference in Porosity

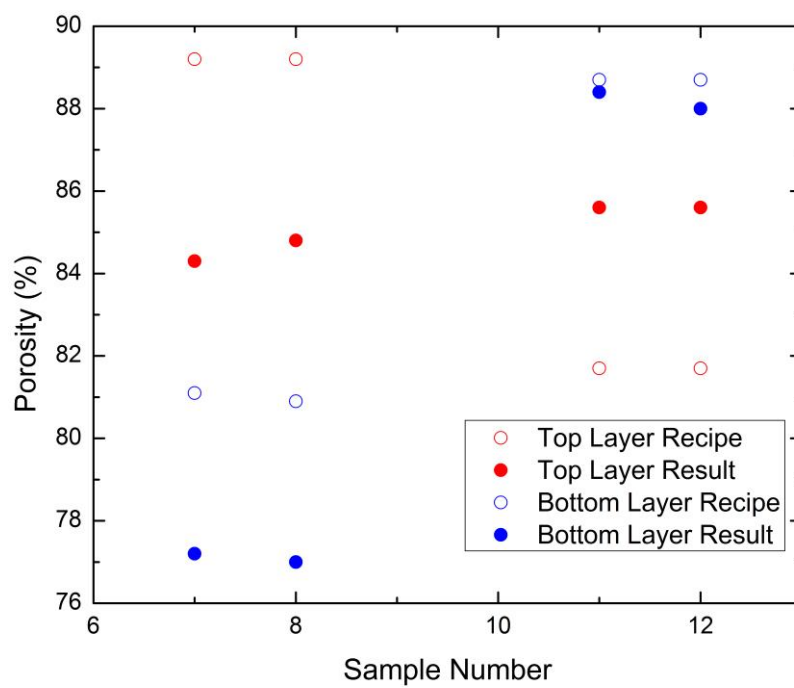


Figure 3.4 Double Layer Samples: Difference in Porosity

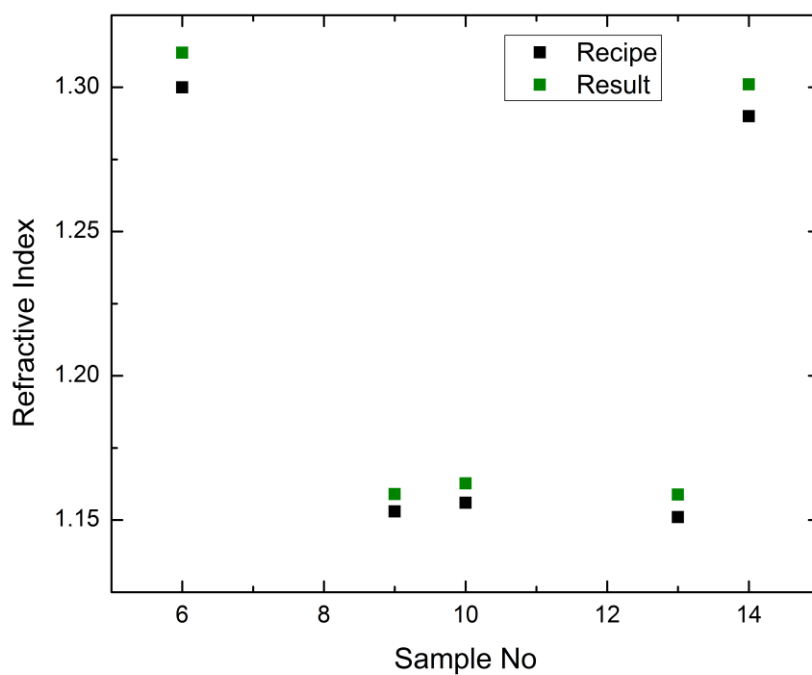


Figure 3.5 Single Layer Samples: Difference in Refractive Index

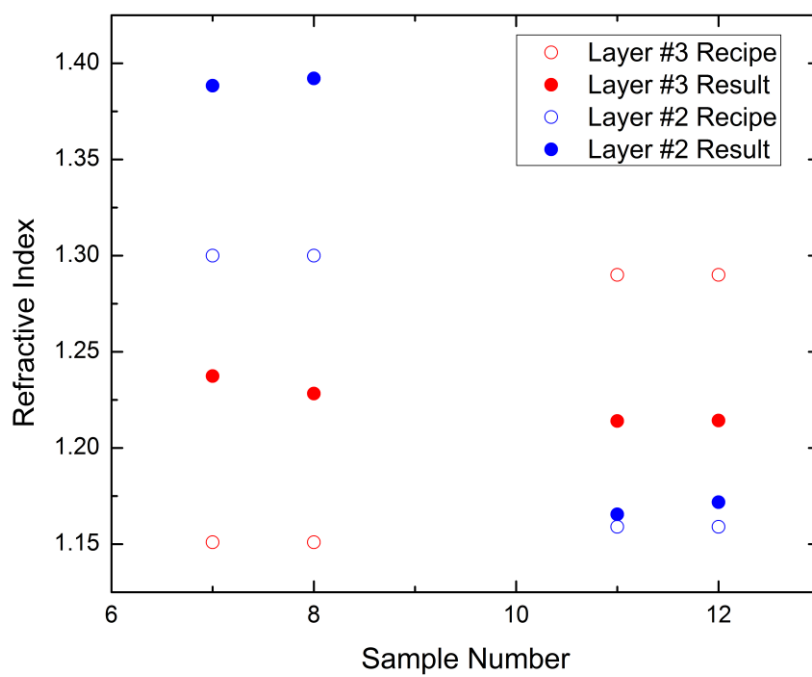


Figure 3.6 Double Layer Samples: Difference in Refractive Index

3.4 LESSONS LEARNED

- **A larger z value** yields a higher refractive index and more dense sample.
- **Particle impact velocity** can affect a thin-film's thickness and density [9].
- **Pressure Readings** *must* remain consistent when creating a batch of samples. Record these readings, and all other Deppy settings, for the sake of experiment repeatability.

CHAPTER 4: ELLIPSOMETRY ANALYSIS

4.1 HOW IT WORKS: ELLIPSOMETER

Ellipsometry measures the change in the polarization of light as it reflects or transmits from a surface. This polarization change is represented with two values: amplitude ratio, Ψ (psi), and phase difference, Δ (delta) [15, 16]. Psi, the ratio of amplitude diminutions, ranges from zero to 90° [17]. Delta is calculated as the phase difference before minus the phase difference after reflection [17]. Delta values range from either zero to 360° , or -180° to $+180^\circ$. The psi and delta values depend on the thickness and optical properties of the material, which ellipsometry analysis methods determine. Ellipsometry can also be used to “characterize composition, crystallinity, roughness, doping concentration, and other material properties associated with a change in optical response” [15].

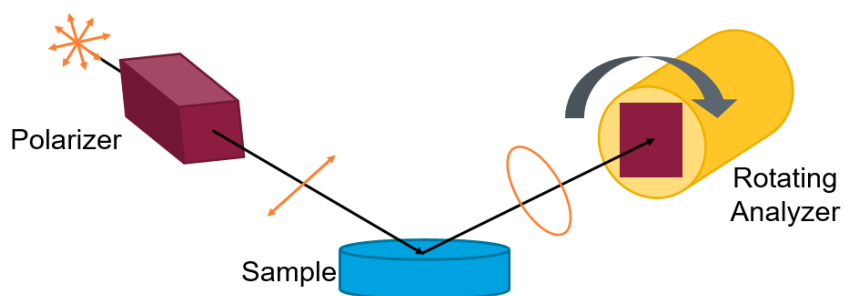


Figure 4.1 Digital Model of M-2000 J.A. Woollam Co. Ellipsometer

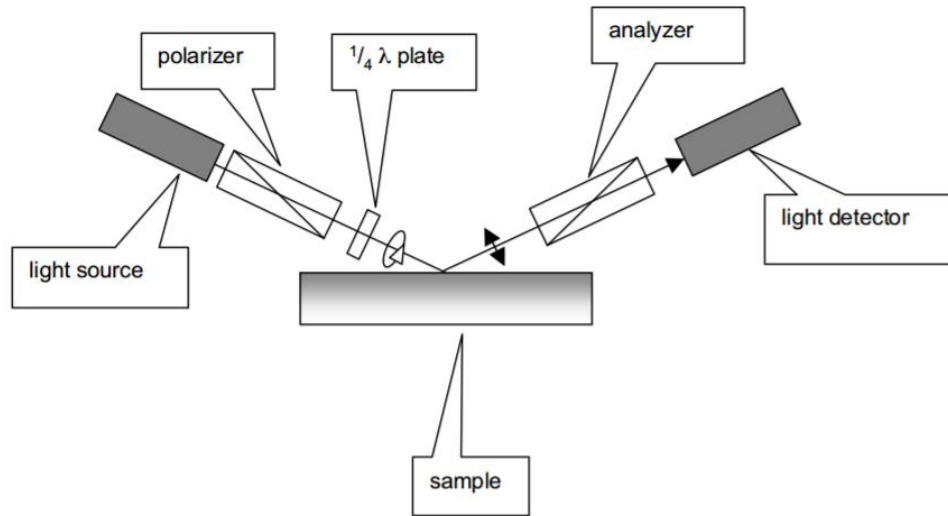


Figure 4.2 Nulling Ellipsometer Schematic [16]

4.2 METHODS

Ellipsometry data collection and analysis methods were used to observe the changes of polarization of light when it reflects off a surface. However, since the silicon nanoparticle optical coatings were exposed to the air, the data must also have accounted for environmental conditions and potential error. This is why the first layer is an intermediate native oxide layer. Using native oxides “as the technology for preparation of ultrathin layers” will yield higher efficiency solar cells because the “deposited dielectric has a common element with the base semiconductor” (silicon nanoparticles are being deposited on top of a silicon wafer) [18].

In the ellipsometry software, CompleteEASE, each layer includes both silicon nanoparticles and air. The Effective Medium Approximation (EMA) and Bruggeman models calculated thicknesses of 102 nm to 328 nm, and porosities of 77% to 89%, depending on the coating.

4.3 RESULTS

The screenshot below illustrates the ellipsometry software analysis of a silicon nanoparticle monolayer (single layer), sample 6. Recall that sample 6 is a dense sample, with a high refractive index and lower porosity.

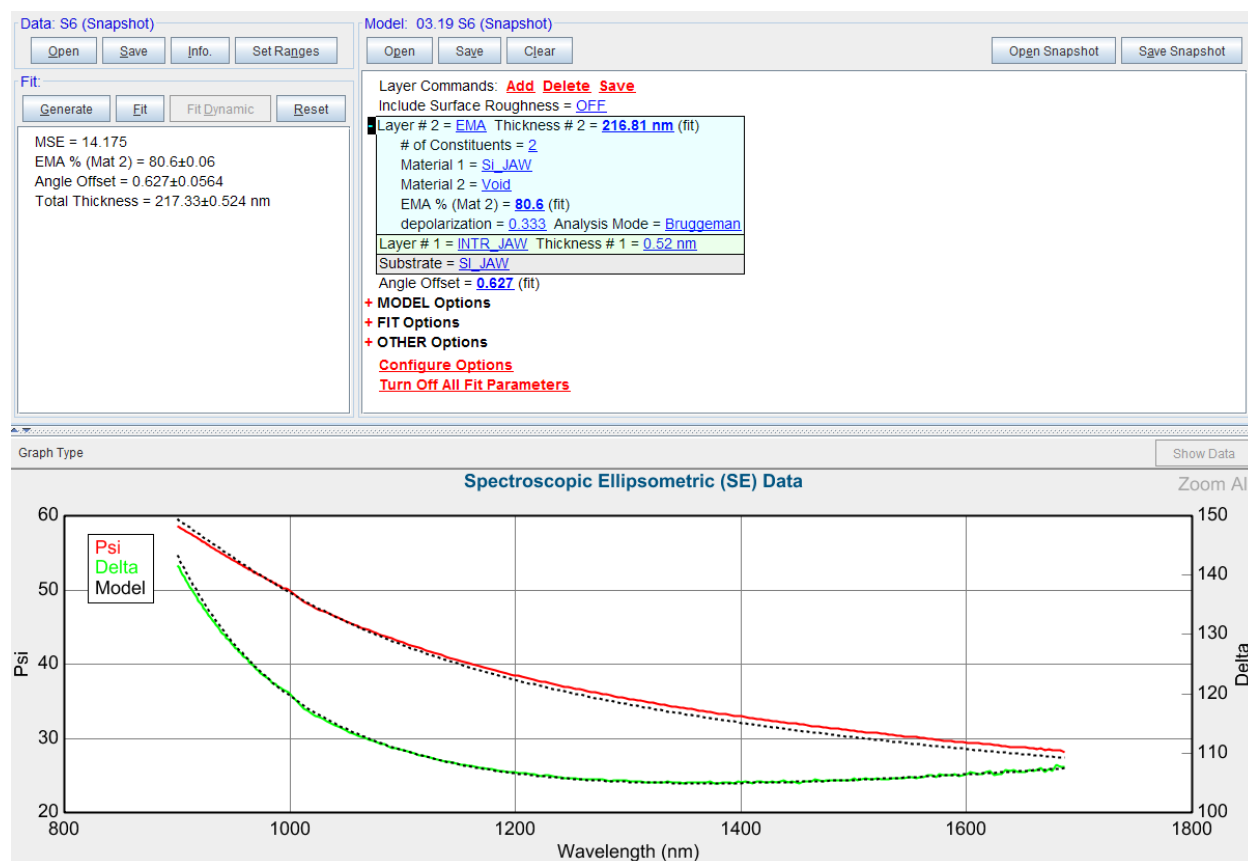


Figure 4.3 Ellipsometry Analysis of Silicon Nanoparticle Monolayer

For all single-layer samples, the model consists of a substrate (silicon), layer #1 (intermediate layer for native oxide), and layer #2 (EMA of silicon nanoparticles and air).

The screenshot below illustrates the ellipsometry software analysis of a silicon nanoparticle multi-layer (double layer), sample 11. Recall that sample 11 is a porous layer stacked on top of a dense layer.

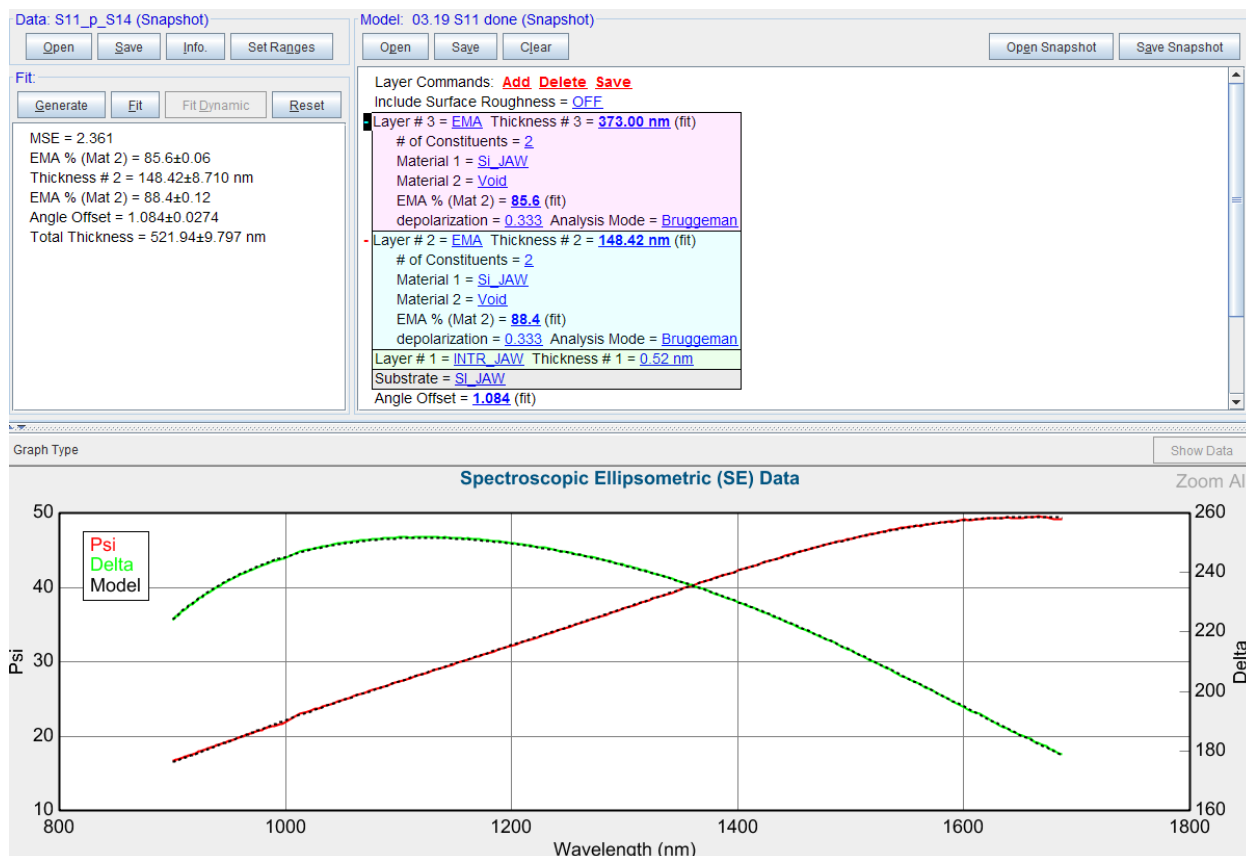


Figure 4.4 Ellipsometry Analysis of Silicon Nanoparticle Multi-Layer

For all multi-layer samples, the model consists of a substrate (silicon), layer #1 (intermediate layer for native oxide), layer #2 (EMA of silicon nanoparticles and air), and layer #3 (EMA of silicon nanoparticles and air). Layers 2 and 3 will have different performance parameters (thicknesses, porosities, and refractive indices).

The tables below list the performance parameters for each sample, including expected values (unshaded cells) and result values (shaded cells).

Sample	6	7	8	9	10	11	12	13	14
Layer 2, Si Nano-particles	215.00 nm	201.00 nm	201.00 nm	205.00 nm	205.00 nm	208.00 nm	210.00 nm	215.00 nm	223.00 nm
Layer 3, Si Nano-particles		215.00 nm	215.00 nm			223.00 nm	223.00 nm		
Layer 2, Si Nano-particles	216.81 nm	127.68 nm	102.48 nm	204.54 nm	204.11 nm	128.42 nm	185.20 nm	214.45 nm	221.82 nm
Layer 3, Si Nano-particles		95.13 nm	125.05 nm			373.00 nm	328.35 nm		

Table 4.1 Thickness: Expected versus Result (shaded)

Sample	6	7	8	9	10	11	12	13	14
Layer 2, Si Nano-particles	80.8	81.1	80.9	89.1	88.9	88.7	88.7	89.2	81.7
Layer 3, Si Nano-particles		89.2	89.2			81.7	81.7		
Layer 2, Si Nano-particles	80.6	77.2	77.0	88.7	88.5	88.4	88.0	88.8	81.1
Layer 3, Si Nano-particles		84.3	84.8			85.6	85.6		

Table 4.2 Porosity: Expected versus Result (shaded)

Sample	6	7	8	9	10	11	12	13	14
Layer 2, Si Nano-particles	1.3	1.3	1.3	1.153	1.156	1.159	1.159	1.151	1.29
Layer 3, Si Nano-particles		1.151	1.151			1.29	1.29		
Layer 2, Si Nano-particles	1.312	1.388	1.392	1.159	1.163	1.166	1.172	1.159	1.301
Layer 3, Si Nano-particles		1.237	1.228			1.214	1.214		

Table 4.3 Refractive Index: Expected versus Result (shaded)

The tables below tabulate the difference between result and expected values, for each performance parameter. The yellow shading indicates a sample made of a dense layer stacked on top of a porous layer. The red shading indicates a sample made of a porous layer stacked on top of a dense layer.

Sample	6	7	8	9	10	11	12	13	14
Layer 2, Si Nano-particles	01.81	-73.32	-98.52	-00.46	-00.89	-79.58	-24.80	-0.55	-01.18
Layer 3, Si Nano-particles		-119.87	-89.95			150.00	105.35		

Table 4.4 Thickness Difference: Result - Expected

Sample	6	7	8	9	10	11	12	13	14
Layer 2, Si Nano-particles	-0.2	-3.9	-3.9	-0.4	-0.4	-0.3	-0.7	-0.4	-0.6
Layer 3, Si Nano-particles		-4.9	-4.4			3.9	3.9		

Table 4.5 Porosity Difference: Result - Expected

Sample	6	7	8	9	10	11	12	13	14
Layer 2, Si Nano- particles	0.0125	0.0884	0.0921	0.0063	0.0069	0.0065	0.0128	0.0078	0.0113
Layer 3, Si Nano- particles		0.0864	0.0773			-0.0760	-0.0757		

Table 4.6 Refractive Index Difference: Result - Expected

4.4 CONCLUSION

There are two different models being compared: dense on top of porous (samples 7, 8) and porous on top of dense (samples 11, 12). Samples 11 and 12 have smaller differences than samples 7 and 8 in all performance parameters, except for the top layer thicknesses. This means that the porous on top of dense model can be replicated and perform to expected standards better than the dense on top of porous model.

4.5 LESSONS LEARNED

- **Use EMA** when a layer has mixed components (a solid material and air).
- **Restrict the wavelength** to 900 - 1700 [3].
- **Observe alternate models** to see their parameter uniqueness fit. This might help identify parameters to modify to reduce the MSE value [19].
- **An accurate model** will have an MSE value of less than 20, ideally less than 10.

CHAPTER 5: SPECTROPHOTOMETRY ANALYSIS

5.1 HOW IT WORKS: SPECTROPHOTOMETER

A spectrophotometer measures reflectance and transmittance of a sample. From these measurements, the software can determine absorbance of a sample. The device functions as so:

1. A lamp is the source of light. The beam of light strikes the diffraction grating. The grating “separates the light into its component wavelengths. The grating is rotated so that only a specific wavelength of light reaches the exit slit” [20].
2. The light hits the sample.
3. The detector will measure the reflectance or transmittance of the sample, whichever property was indicated by the user.

Reflectance is the measurement of light that the sample reflects. Transmittance is the amount of light that travels through the sample and strikes the detector. Absorbance is the measurement of light that the sample absorbs [20].

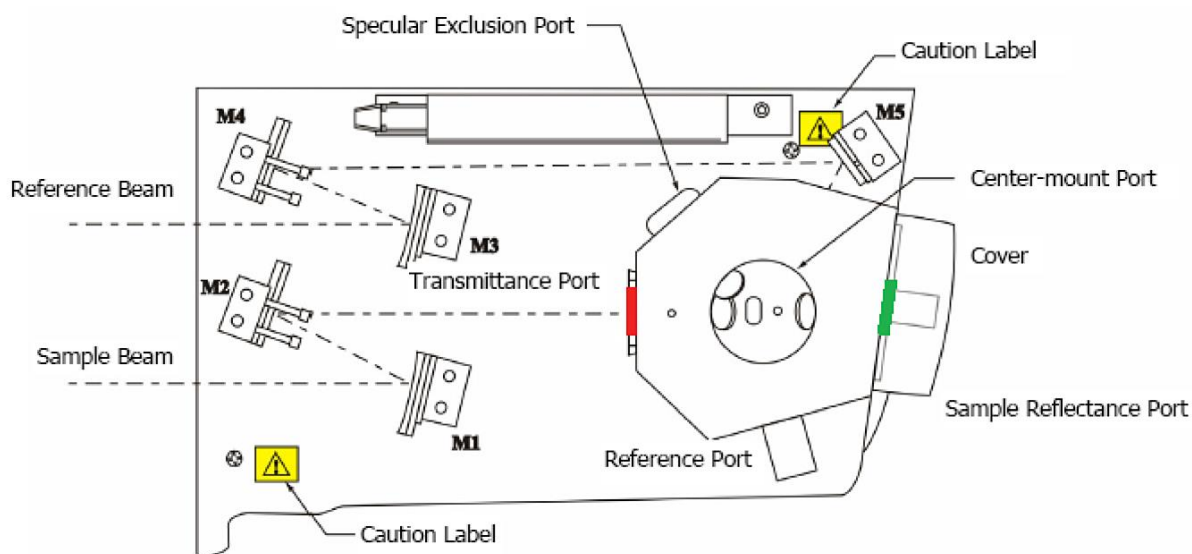


Figure 5.1 Top Down View of the Lambda 950 Spectrophotometer. The red area is where transmission of a material occurs, and the green area is where reflectance occurs [21].

5.2 METHODS

The Lambda 950 Spectrophotometer was used to take reflectance measurements for each sample. All light spectra were corrected “for the reflectance of the reference material (light spectral reference), as well as the dark level (0%R) of the sphere (dark spectral reference)” [21]. The Labsphere Calibrated Spectralon Standard was used to generate Absolute %R with an integrating sphere. Dark reference corrections were made before sample analysis. After all adjustments and corrections were made, the reflectance data was collected.

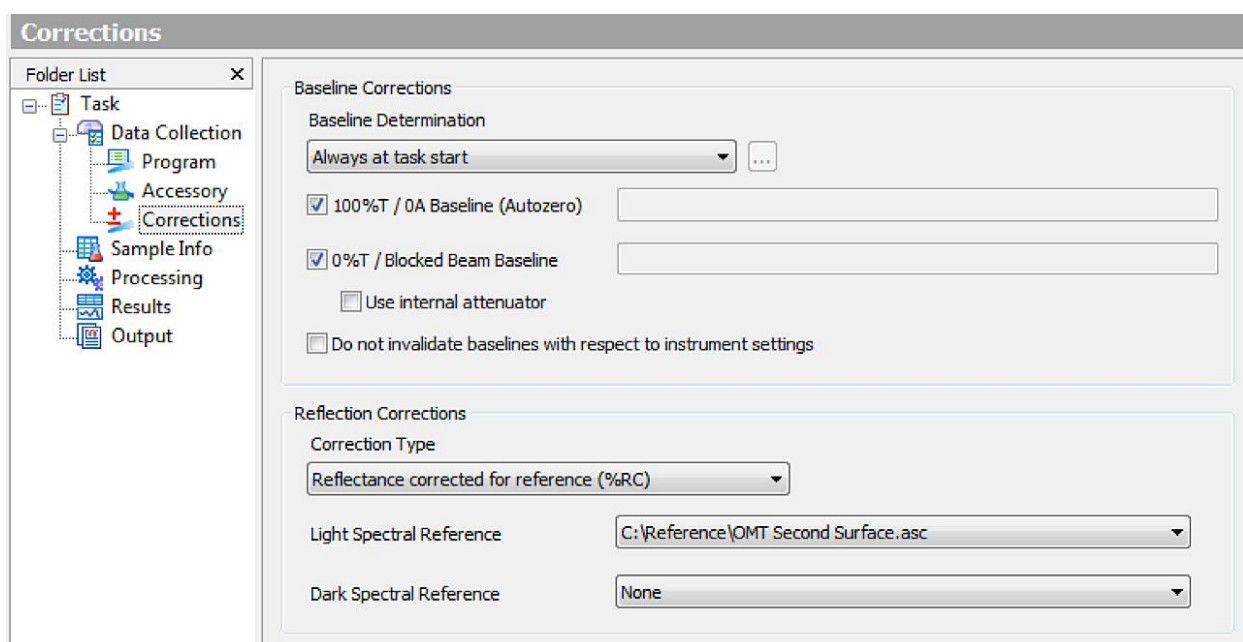


Figure 5.2 Reflectance Correction Settings in the Integrating Sphere

5.3 RESULTS

The graph below illustrates the reflectance of single layer samples in the wavelength range of 350 to 1600 nm.

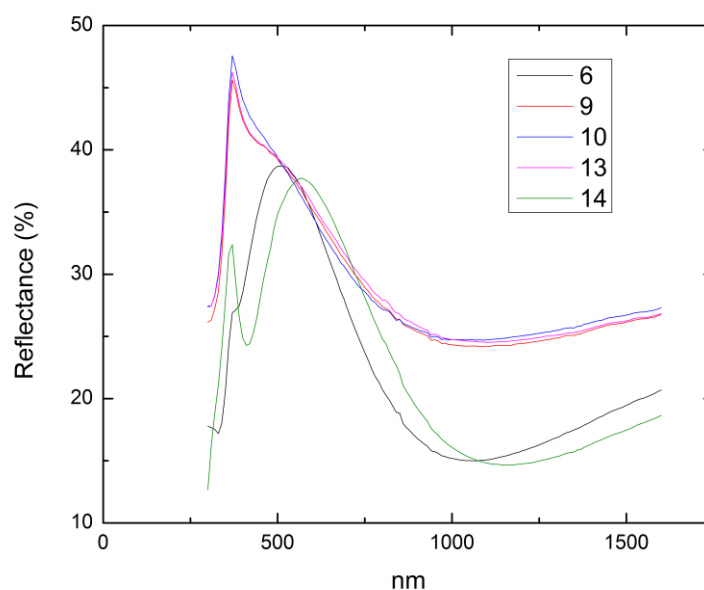


Figure 5.3 Silicon Nanoparticle Monolayer Reflectance Values

The graph below illustrates the reflectance of multi-layer samples in the wavelength range of 350 to 1600 nm.

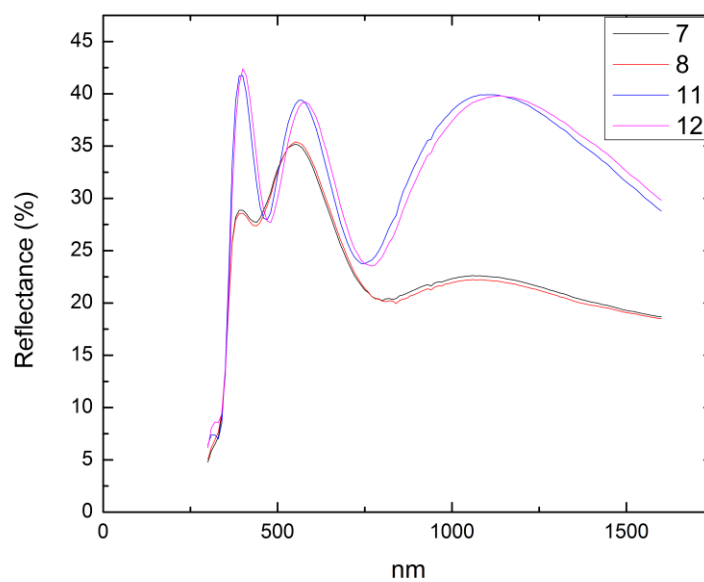


Figure 5.4 Silicon Nanoparticle Multi-Layer Reflectance Values

Recall that the scope of this experiment evaluates performance parameters within the wavelength range of 950 to 1200 nm [5]. The average reflectance values of dense, single layer samples within scope range are 15.28% (sample 6) and 15.38% (sample 14). The average reflectance values of porous, single layer samples within scope range are 24.32% (sample 9) and 24.68% (sample 13). The average reflectance values of dense on top of porous (multi-layer) samples are 22.35% (sample 7) and 21.97% (sample 8). The average reflectance values of porous on top of dense (multi-layer) samples are 39.09% (sample 11) and 38.60% (sample 12).

5.4 CONCLUSION

The highest reflectance values were achieved with the porous on top of dense multi-layer model (samples 11 and 12). The lowest reflectance values were achieved with a dense, single layer model (samples 6 and 14).

Samples with greater thicknesses had higher reflectance values (11 and 12 had greater reflectance values than 7 and 8). Multi-layer samples (7, 8, 11, 12) generally had higher reflectance values than their single layer (6, 9, 10, 13, 14) counterparts. The porous on top of dense multi-layer model (11 and 12) had the lowest porosity and highest thickness of all the models in this experiment. It is clear that the porosity, thickness, and number of layers affects reflectance values.

5.5 LESSONS LEARNED

- **Set the Ordinate Mode** to reflectance or transmittance, whichever value is being measured.
- **Always set corrections**, or correct the data file after measurement collection.

- **Update the InGaAs Setting** to 11.00 [22, 23].
- **Autozero** with either a dark or light sample.
- **Measure an uncoated wafer** to serve as a reference for the coated wafers.
- **Double check that the sample covers the entire reflection port** before data collection.
- **If the sample does not cover the entire reflection port**, use the appropriate aperture to reduce the gap. Adjust the mirrors as necessary.

CHAPTER SIX: FUTURE WORK

The data of this experiment explored only single layer and double layer silicon nanoparticle optical coatings. While the double layer models satisfied the experiment objectives, three, four, or five layer models were not considered. Future work entails the virtual modeling, deposition, and analysis of three, four, and five layer models.

Based on the results from this experiment, a starting point for a models with at least three layers might be to alternate between dense and porous layers. For example, a four layer model would consist of the following layers, from bottom to top: dense, porous, dense, porous. The goal remains the same: create an optical coating model that has five or fewer layers with the maximum reflectance possible between 950 and 1200 nanometers for normally incident light.

CHAPTER SEVEN: CONCLUSION

The primary goal of this work was to design an optical coating model that had five or fewer layers with the maximum reflectance possible between 950 and 1200 nanometers for normally incident light.

The main contributions of the work are:

1. The porous on top of dense model had smaller differences between expected (recipe) and result values. This model can be created and is proven to perform to expected standards better than other tested models.
2. The porous on top of dense model yielded the highest reflectance values: 39.09% (sample 11) and 38.60% (sample 12).
3. The dense, single layer model yielded the lowest reflectance values: 15.28% (sample 6) and 15.38% (sample 14).

The porous on top of dense model meets the goal. It has the highest reflectance values of all models tested in this experiment. Its performance parameters (thickness, porosity, and refractive index) have the smallest discrepancies between expected and result values, proving its accuracy. Based on the results of this experiment, the porous layer should always be on top of the dense layer, with respect to silicon nanoparticle multi-layer optical coatings.

REFERENCES

- [1] D. M. Powell *et al.*, “Crystalline silicon photovoltaics: a cost analysis framework for determining technology pathways to reach baseload electricity costs,” *Energy Environ. Sci.* Rep. 5874, Jan. 2012, vol. 5.
- [2] Arizona State University. *Research Themes* [Online].
Available: <https://engineering.asu.edu/research/research-themes/>
- [3] *Macleod: Optical Thin Films*, January 3, 2013 ed., Thin Film Center Inc., Tucson, AZ, 2013.
- [4] *Military Standardization Handbook: Optical Design*, October 5, 1962 ed., Defense Supply Agency, Washington, D.C., 1962.
- [5] L. Remache *et al.* (2016). *Optical properties of porous Si/PECVD SiNx:H reflector on single crystalline Si for solar cells* [Online]. Available DOI: 10.1515/msp-2016-0054
- [6] L. Mangolini *et al.*, “High Yield Plasma Synthesis of Luminescent Silicon Nanocrystals,” High Temperature and Plasma Lab., Univ. Minnesota, Minneapolis, MN, Nano Letters no. 4. Jan. 2005, vol. 5.
- [7] R. Hummel, “The Optical Constants,” in *Electronic Properties of Materials*, 4th ed. New York, NY: Springer Science+Business Media, LLC, 2011, ch. 10.
- [8] University of Toledo. (2012, Feb. 2). *The p-n Homojunction* [Online]. Available: http://astro1.panet.utoledo.edu/~relling2/teach/archives/6980.4400.2012/20120202_PV_Junctions.pdf
- [9] P. Firth. (2016, Oct. 31). Deppy. [YouTube video]. Available: <https://www.youtube.com/watch?v=0G2-cvOmS2I>. Accessed Mar. 27, 2017.
- [10] J. Meier, R. Flückiger, H. Keppner, A. Shah, *Appl. Phys. Lett.* 65 (1994) 860.
- [11] J. Meier, S. Dubail, R. Flückiger, D. Fischer, H. Keppner, A. Shah, in: *Proceedings of the*

- 1st WCPEC, 1994, pp. 409.
- [12] A. Shah, P. Torres, R. Tscharnner, *et al.*, Science 285 (1999) 693.
- [13] J. Meier, E. Vallat-Sauvain, S. Dubail, *et al.*, Solar Energy Mater. Solar Cells 66 (2001) 73.
- [14] J. Bailat, E. Vallat-Sauvain, *et al.*, “Influence of substrate on the microstructure of microcrystalline silicon layers and cells,” Institut de Microtechnique, Université de Neuchâtel, Neuchâtel, Switzerland, Journal of Non-Crystalline Solids 299-302, 2002, 1219-1223.
- [15] J.A. Woollam. (2017). *What is Ellipsometry?* [Online]. Available:
<https://www.jawoollam.com/resources/ellipsometry-tutorial/what-is-ellipsometry>
- [16] D. Hung. (2008, Jan. 10). *Ellipsometry Basics* [Online]. Available:
http://www.sun-way.com.tw/Files/DownloadFile/Ellipsometry_basics.pdf
- [17] H. Tompkins. *Spectroscopic Ellipsometry* [Online]. Available:
<https://www.aps.org/units/fiap/meetings/presentations/upload/tompkins.pdf>
- [18] R. Singh, *et al.*, “Review of Conductor-Insulator-Semiconductor (CIS) Solar Cells,” Energy Conversion Devices, Inc., Troy, MI, Solar Cells, no. 3, 1981, pp. 95-148.
- [19] *CompleteEASE Data Analysis Manual*, 3.65 ed., J.A. Woollam Co., Inc., Lincoln, NE, 2008.
- [20] Learning Solutions Team. (2011). *How does a spectrophotometer work?* [Online].
 Available: <http://www.lsteam.org/projects/videos/how-does-spectrophotometer-work>
- [21] *UV/Vis Spectroscopy*, PerkinElmer Inc., Shelton, CT, 2013.
- [22] M. A. Green, K. Emery, Y. Hishikawa, *et al.*, “Solar cell efficiency tables (version 42),” Prog. Photovoltaics, Res. Appl., vol. 21, pp. 827–837, 2013.
- [23] I. Almansouri, A. Ho-Baillie, S. P. Bremner, *et al.*, “Supercharging Silicon Solar Cell

Performance by Means of Multijunction Concept,” IEEE Journal of Photovoltaics, Vol. 5, No. 3, 2015.